Simplified flood evacuation simulation in outdoor built environments. Preliminary comparison between setup-based generic software and custom simulator

POSTPRINT OF Quagliarini E, Bernardini G, Romano G, D'Orazio M (2022) Simplified flood evacuation simulation in outdoor built environments. Preliminary comparison between setup-based generic software and custom simulator. Sustainable Cities and Society 81:103848. https://doi.org/10.1016/j.scs.2022.103848

Highlights.

- We investigate evacuation simulation in flooded outdoor built environments.
- We compare a generic and a custom simulation model based on a microscopic approach.
- We set a generic simulator up to reproduce flood-related behaviors.
- Simulators are applied to an idealized literature-based case study, including comparisons with real-world data.
- Results seem to encourage the proposed generic simulator setup.

Abstract. Floods are among the most destructive sudden-onset disasters affecting worldwide communities and society. Pedestrians can be forced to evacuate affected areas thus being exposed to multiple risks. Outdoor built environment flood risks analyses should be performed through rapid, easy, and sustainable tools to speed up and support risk assessment and mitigations. Custom evacuation simulators have been developed, but are generally used in research, are not user-friendly, and need high-level training. On the contrary, generic (e.g. commercial) software tools seem to be more suitable for low-trained technicians but should be modified to include human behaviors effects, especially considering the evacuation, when people's peculiar choices depend on interactions with floodwaters and built environment layout/composing elements. This work provides preliminary setups of a generic software tool to perform quick and sustainable assessments of pedestrians' flood safety in outdoor spaces, using an easy-to-apply no-code modification approach to include flood peculiar behaviors. Simulation outputs of the setup-based generic software are compared with a custom simulator relying on the same modelling approach, and with real-world observations, using an idealized literature-based outdoor scenario. Results provide the best setup of the generic software to reliably represent evacuation phenomena, thus encouraging its future application also by local authorities.

Keyword. Urban flood; flood evacuation; pedestrians' evacuation; behavioral model; social force model; evacuation simulation; urban built environment; risk assessment.

1. Introduction

According to the UNDRR, “a sudden-onset disaster is one triggered by a hazardous event that emerges quickly or unexpectedly”[1]. Between them, worldwide, floods are the most common and devastating threats for our cities and society, affecting each year more individuals than any other disaster (European Commission, 2017; Gu, 2019; Young & Jorge Papini, 2020).

Thus, reliable but quick analyses are necessary to promote flood risk assessment actions and based on them effective risk-mitigation strategies in the urban Built Environment (BE) (Chang et al., 2021; Gandini et al., 2020, 2021; Wan Mohtar et al., 2020), such as early warning systems, drainage, and floodwater storage systems in the BE, rescuers’ actions management and evacuation planning in terms of gathering areas positioning, safe path identification and implementation of handrails and platforms to support pedestrians in evacuation. In this context, analyses concerning the outdoor spaces in the urban BE, such as streets, squares, parks, and other open spaces in the urban BE (French et al., 2019; Puchol-Salort et al., 2021; Rezende et al., 2019), seem to have a paramount relevance (Bernardini, Postacchini, et al., 2017; Fan et al., 2018; Jamrussri & Toda, 2018; Li et al., 2019; Matsuo et al., 2011; Najafi et al., 2021; Paquier et al., 2015; Piyumi et al., 2021). Outdoor spaces shape the urban layout, thus affecting the flood spreading in it (Bazin et al., 2017; Beretta et al., 2018; Najafi et al., 2021; Piyumi et al., 2021; Puchol-Salort et al., 2021; Rezende et al., 2019; Zhuo & Han, 2020), and so they are critical environments for the safety of the BE users, especially during emergency conditions, i.e. in the evacuation process (Bernardini, Camilli, et al., 2017; Kim et al., 2021; Lumbroso & Davison, 2018; Shirvani & Kesserwani, 2021).

Previous works pointed out how risk assessment tasks, related risk mapping actions and evaluations on risk-mitigation strategies should take advantage of simulation models in view of the complexity of the overall system, that comprises, i.e., the flood characterization also depending on climate-change effects, the land use effect, the BE vulnerability, the users’ spatiotemporal dynamics, and the

[1] https://www.undrr.org/terminology/disaster (last access 29/10/2021)

users' behaviors also in emergency conditions (da Silva et al., 2022; Domingo et al., 2021; Dong et al., 2020; Han & Mozumder, 2022; Kim et al., 2021; Lumbroso & Davison, 2018; Najafi et al., 2021; Piyumi et al., 2021).

Recent related works investigate multiple cross-cutting issues (Beretta et al., 2018; da Silva et al., 2022; Domingo et al., 2021; Dong et al., 2020; Han & Mozumder, 2022; Najafi et al., 2021; Piyumi et al., 2021), such as: failures of channels, networks, and infrastructures; rainfall and storm-surge simulations; urban layout and outdoor spaces configuration effects on risk and floodwater spreading; demographic forecasting; changes in land-use patterns. Efforts to include evacuation and users' behaviors modelling in flood conditions have been provided (Bernardini, Postacchini, et al., 2017; Kim et al., 2021; Li et al., 2019; Lumbroso & Davison, 2018). Such models allow evaluating the effects of interactions between the pedestrians, the floodwater conditions, and the surrounding BE on users' risks and possible casualties, mainly based on the effects of floodwater depth and speed on pedestrians' speed reduction, buoyancy phenomena, and body failure (Ashley & Ashley, 2008; Bernardini, Postacchini, et al., 2017; Cox & Shand, T.D.Blacka, 2010; Dias et al., 2021; Samany et al., 2021; Shirvani et al., 2020; Takagi et al., 2016). Some models also included the perception of unmovable obstacles as safe elements for pedestrians walking through floodwaters in an urban BE that can alter the pedestrians' trajectories because of attraction phenomena (Bernardini, Postacchini, et al., 2017). In particular, according to the analysis of real-world videotapes concerning flood evacuation, pedestrians prefer moving towards and near walls and fences (preferred distance of about 1m to 2m, with an experimental considered limit of 3m) to gain support and handle on them while walking.

In view of the above-mentioned interactions between the pedestrians, the floodwater, and the surrounding BE, microscopic models rather than macroscopic approaches should be preferred, since they are able to represent the specific individual-scale interactions in the evacuation process (Jebrane et al., 2019). Such a microscopic approach has been adopted by several flood evacuation simulators proposed according to different modelling methodologies (e.g. cellular automata, social force models)

(Bernardini et al., 2021; Bernardini, Postacchini, et al., 2017; Kim et al., 2021; Li et al., 2019; Lumbroso & Davison, 2018; Matsuo et al., 2011; Shirvani et al., 2020; Shirvani & Kesserwani, 2021). Efforts to test these simulation tools in relevant conditions have been provided, including comparisons with real-world observations and moving towards the verification and validation of models (Bernardini, Postacchini, et al., 2017; Li et al., 2019; Ronchi et al., 2013; Ronchi, 2020). Then, these simulation tools have been applied for preliminary evaluations of the effectiveness of emergency solutions (Bernardini, Postacchini, et al., 2017; Bodoque et al., 2016; Dai et al., 2020; Jamrussri & Toda, 2018; Jia et al., 2016; Kolen & van Gelder, 2018; Mignot et al., 2019), especially those directly aimed at helping people when structural solutions fail/miss or massive events occur (e.g., evacuation plans, safe areas identification). However, such simulators are generally considered as custom software, mainly developed for research purposes, and characterized by a high complexity level in terms of use, functionality, and interoperability that could slow down (or impede) crucial analyses for the risk assessment, especially considering applications to real-world BEs performed by Local Authorities technicians, who can have a low training level on the matter.

Generic evacuation simulation tools, on the contrary, represent a powerful solution to improve a sustainable application of evacuation simulation tools in real-world contexts, since they are widely implemented in more user-friendly software, especially considering commercial ones. They are oriented towards general-purpose evacuation simulation or fire scenarios and use behavioral and motion quantities from related databases (Bosina & Weidmann, 2017; Ronchi, 2020; Shi et al., 2009). Their general verification and validation process has been provided according to standard testing conditions (Ronchi et al., 2013). Nevertheless, generic software needs adequate modifications to represent flood-related behaviors. To solve this issue in a quick, easy-to-apply, standard-based and so sustainable way, specific software setups can be developed adopted, thus avoiding complexity-increasing operations on the source code or the implementation of dedicated plug-ins and additional tools.

Within this framework, for the first time, this work tries to provide preliminary, innovative support to technicians and safety designers on how to adapt a generic software to carry out quick and sustainable assessments of the pedestrians' flood safety in outdoor spaces. A proper setup of an existing generic software based on microscopic evaluation modelling (MassMotion Guide, 2020), generally used for indoor evacuation analysis purposes, has been provided to include main pedestrians' flood behaviors, thus focusing on a few simple setup parameters. Then, reliability analyses of such a setup-based generic model have been provided according to literature standards and using a simple testing scenario (a linear and flat street), by analyzing different configurations on the selected setup parameters (Bernardini, Postacchini, et al., 2017; Li et al., 2019; Ronchi et al., 2013; Ronchi, 2020). First, comparisons with an existing custom flood simulation software have been provided. Since the selected generic software adopts a Social Force Model (SFM) approach for the evacuation simulation (Helbing et al., 2000), the selected custom simulator (Flooding Pedestrians' Evacuation Dynamics Simulator - FlooPEDS) (Bernardini, Postacchini, et al., 2017) is similarly founded on the same approach. FlooPEDS has been also developed and preliminarily validated according to real-world observations for flood evacuation purposes, as well as applied to real-world contexts for the analysis of risk-mitigation solutions (Bernardini et al., 2021). Second, additional comparisons with observations on pedestrians' motion from real-world floods are also used to evaluate the setup-based generic software reliability (Bernardini, Camilli, et al., 2017).

The testing scenario is quite simple and concerns stationary flood conditions where small compact groups of pedestrians are evacuating. Nevertheless, as in general aims of standard testing conditions for verification and validation of evacuation simulators (Bernardini, Postacchini, et al., 2017; Li et al., 2019; Ronchi et al., 2013; Ronchi, 2020), if the comparison is not effective in such a simple scenario, more sensible differences between the simulators will surely appear in more complex outdoor BE or conditions. The authors are also aware that this kind of analysis cannot be always defined as a fair and exhaustive comparison, because of the peculiarities of the modelling logic and the specific conditions of real-world floods. Anyway, they can roughly and preliminarily evaluate possible differences and behavioral uncertainties in simulation outputs typical of the considered disaster (e.g. evacuation timing, trends of distances between pedestrians, and unmovable obstacles) in different approaches.

2. Methods

This work is organized in the following steps, as described in the following methodological sub-sections.

First, the criteria for generic software setup are provided to quickly replicate main flood-affected evacuation behaviors in outdoor scenarios (Section 2.1). They are implemented in the selected generic simulator (Helbing et al., 2000), and the related features and modelling logic are compared with those of the custom simulator (FlooPEDS) (Section 2.2). Then, a scenario is selected according to previous works (Bernardini, Postacchini, et al., 2017) to apply the setup-based generic simulator and the custom one (FlooPEDS) for comparison purposes (Section 2.3). Different setup solutions of the generic simulator are tested, thus allowing us to check the factors that can alter the expected simulation outputs with respect to the custom simulator evacuation and the real-world observations (Section 2.4). Simulation results of the two software are compared through the main significant outputs to be evaluated for the flood evacuation, and additional analyses concerning observations from real-world flood events are provided for the setup-based generic simulator (Section 2.5).

2.1. Basic criteria to replicate pedestrian behaviors

The characterization of the pedestrian behaviors in flood in the generic software is based on the following main drivers from literature review: (1) the evacuation speed v_i [m/s], (2) the body instability, and (3) the attraction towards unmovable obstacles. For each modelling assumption, advantages and implementation issues concerning the comparison process and the full-scale application are discussed in the following.

Concerning v_i, Equation 1 (Bernardini, Camilli, et al., 2017) calculates the experimental-based evacuation speed for given floodwater depth D_f [m] and speed v_f [m/s] (g is the gravitational acceleration [m^2/s]). The higher D_f and v_f, the lower the evacuation speed v_i. Additional differences in motion speeds depending on age, motion abilities and gender can be considered modifying the numerical parameters in Equation 1 (Lee et al., 2019).

$$v_i = 0.52\left(\frac{D_f \cdot {v_f}^2}{g} + \frac{{D_f}^2}{2}\right)^{-0.11} \quad (1)$$

Concerning body instability, general consolidated thresholds to these problems refer to $D_f * v_f \geq 1.2$ m^2/s or $v_f \geq 3.0$m/s, and, in the case of still water, $D_f \geq 1.2$m, which provokes buoyancy (Cox & Shand, T.D.Blacka, 2010).

Previous works pointed out the possibility to consider homogeneous floodwater conditions for the street/square in the BE, or a part of it (e.g. the outdoor part between two consecutive crossroads), thus dividing the space in a grid (Bernardini et al., 2021; Kim et al., 2021; Lumbroso & Davison, 2018; Shirvani & Kesserwani, 2021). This choice can be sustainable since it reduces the implementation and computational complexity of local D_f and v_f effects on v_i and body stability. According to such an approach, in a full-scale application scenario, the motion space can be divided into different areas to represent streets/squares in the BE or a part of them (as for floors in case of building evacuation simulators (MassMotion Guide, 2020)). Each area can be characterized by D_f and v_f values which are constant in the area, but dynamic over the simulation time, depending on the floodwater spreading simulation (Beretta et al., 2018; Bernardini et al., 2021; Dai et al., 2020; Piyumi et al., 2021).

Concerning the attraction towards unmovable obstacles, literature data concerning real-world observations of pedestrian behaviors along flooded streets noticed that pedestrians prefer to stay closer than about 3m from building walls, fences, and other continuous and unmovable elements in any case (Bernardini, Postacchini, et al., 2017).

2.2. Custom and generic simulators: modelling logic

FlooPEDS is used as the custom reference simulator (Bernardini, Postacchini, et al., 2017) since it includes all the main criteria provided by Section 2.1. FlooPEDS combines a module to simulate flood hydrodynamics based on Nonlinear Shallow Water Equations (NSWE) (Bazin et al., 2017; Soares-Frazão et al., 2008), and a module to simulate pedestrians' evacuation based on the SFM approach, thus pursuing a microscopic approach. The NSWE and the SFM-based modules of FlooPEDS work in series, with no back interaction of pedestrians on the water flows. Since, in this work, the core of the comparison with the generic software concerns the pedestrians' evacuation model, the hydrodynamic one is ignored here.

MassMotion 10.6[2] is used as the generic simulator to be modified according to Section 2.1 criteria. In general terms, the two models consider that the simulated pedestrians (in MassMotion, *agents*) move in 2-D planes, from an initial position to reach intermediate and final evacuation targets (in MassMotion, *portals* represent both the entrances into the simulation and the pedestrians' destinations). The planes can be divided into one or more areas (in MassMotion, they are the *floors*), depending on the specific D_f and v_f local conditions (hence v_i, as discussed in Section 2.1 and Equation 1). As for FlooPEDS, MassMotion adopts the SFM approach to simulate the microscopic pedestrians' movement (Helbing et al., 2000). The calculation of the evacuation velocity $\overrightarrow{v_i(t)}$ [m/s] (as a vector) for each pedestrian involved in the simulation depends on the sum of repulsive and attractive forces on the pedestrian, according to Equation 2:

$$m_i \frac{\overrightarrow{dv_i(t)}}{dt} = \overrightarrow{O_g(t)} + \sum \overrightarrow{F_{rep,i}(t)} + \sum \overrightarrow{F_{rep,w}(t)} + \sum \overrightarrow{F_{attr,i}(t)} + \sum \overrightarrow{F_{attr,w}(t)} \quad (2)$$

where m_i [kg] is the body mass of the pedestrian, *dt* [s] is the time between two consecutive calculation iterations, $\overrightarrow{O_g(t)}$ [N] is the drive-to-target force depending on the target direction, and the current and desired pedestrian's velocity (and so, it depends on v_i). In Equation 2, the pedestrian is

[2] Tests (randomly selected within the list of the validation scenarios in Section 2) are additionally carried out with MassMotion 9.5.2.2 to compare results with the previous version and no differences are found.

affected by attractive (subscript *attr*) and repulsive (subscript *rep*) forces [N] with the surrounding pedestrians *i* and with the surrounding obstacles *w*. The main difference between the two simulators logics relies on the attractive force between the individual and the unmovable obstacles $\overrightarrow{F_{attr,w}(t)}$. FlooPEDS, unlike the generic simulator, also includes this phenomenon, considering the attraction of elements placed at a distance equal to or lower than 3m (Lakoba et al., 2005). In particular, the attraction force modulus in FlooPEDS is equal to 300N, according to verifications with real-world observations (Bernardini, Postacchini, et al., 2017). The adopted values for the other specific SFM parameters in FlooPEDS simulations are reported by the original verification work (Bernardini, Postacchini, et al., 2017).

In view of the criteria shown in Section 2.1, this work considers stationary floodwater conditions for both the application of FlooPEDS and MassMotion, that is assuming that D_f and v_f do not change over the simulation time. A unique area in terms of D_f and v_f is simulated, thus creating a unique v_i value in the setup process. Maximum (e.g. capped) motion speed v_i are calculated according to Equation 1 so as to adopt a conservative approach in the motion speed estimation, and so in the evacuation timing assessment. As for most of the evacuation simulators, differences between v_i are assigned in a rapid manner using a v_i distribution, and so they could be used to additionally consider different pedestrian typologies. According to the reference work (Bernardini, Postacchini, et al., 2017), v_i in the range 0.85±0.05 m/s (Gaussian distribution) is herein assigned to describe low-medium floodwater levels, e.g. being $(D_f \cdot v_f^2)/g+D_f^2/2 \approx 0.01 m^3/m$.

Non-critical conditions for human body stability are assumed in this work. Indeed, it is considered that the motion-process for a safe evacuation should be carried out avoiding possible major threats due to floodwater (Opper et al., 2010). Thus, all the pedestrians can arrive in a safe area in the simulated scenario, and tests can focus on the motion tasks.

Finally, in the MassMotion setup, the simulated pedestrians are assumed to move along linear paths alongside the building walls/fences, thanking the use of *servers* (MassMotion Guide, 2020). The *servers* are elements already present within MassMotion, and they are useful to model queues and, more in general, to vehiculate the pedestrians' movements and behaviors. Using *servers* to model the pedestrian-unmovable obstacles attract could introduce some simplifications according to Equation 2, i.e. does not consider possible variations in their trajectory due to extraordinary conditions related, for instance, to the presence of floating obstacles or impracticable areas.

2.3. Tested scenario

The setup-based version of MassMotion and FlooPEDS are applied to the same typological scenario for comparison purposes. The tested scenario is quite simple in adherence with the consideration of Section 2.1 and Section 2.2, and it consists of a linear and flat pathway representing a common outdoor BE such as a street, with stationary flood conditions and small compact groups of pedestrians evacuating. This configuration allows focusing on the pedestrians' elementary motion contingencies since constant floodwater conditions are imposed[3]. In this sense, it is representative of a street for a simple but critical layout in urban open spaces and it is also consistent with the IMO (International Maritime Organization) test 1 layout (Ronchi et al., 2013). Indeed, as in the general aims of standard testing conditions for verification and validation of evacuation simulators, if the comparison is not effective in such a simple scenario (that is considering linear trajectory by the pedestrians, stationary environmental conditions over time and space, small groups of pedestrians, flat and linear pathway), more sensible differences between the simulators will surely appear in more complex outdoor BE or conditions (e.g., due to unexpected variability in human behavior, presence of floating obstacles).

In detail, this testing scenario is 17.6m wide and 87m long, with no internal crossroads. Two continuous buildings are considered placed alongside the pathway, one on each pathway side. It hence represents a typical real-world urban built environment, i.e. composed by orthogonal urban fabric, according to previous FlooPEDS testing conditions (Bernardini, Postacchini, et al., 2017). Appendix

[3] There is no influence due to the floodwater direction and so effects of pedestrian-pedestrian and pedestrians-obstacles interactions can be better highlighted.

A resumes the overall details on the setup of the generic software for the scenario implementation, while runs performed with FlooPEDS according to previous works results consider a cad file representing the same scenario.

The following general rules are applied for simulations in the tested scenario reference work for both MassMotion and FlooPEDS (Bernardini, Postacchini, et al., 2017). Tests are carried out by considering compact groups of 10 pedestrians per side starting the evacuation at the same time, to point out the overlapped effects of SFM attractions between the pedestrians themselves, and between the pedestrians and the buildings. The number of simulated pedestrians is provided by considering that the average number of exposed pedestrians (coming from buildings) per square meters of outdoor BE could refer to low-density conditions (LOS A, free circulation, lower than 0.08pp/m^2 (Fruin, 1971)). Such values are consistent with input data on pedestrians' densities from previous works (Samany et al., 2021; Shirvani et al., 2020). Pedestrians are generated at the starting of the pathways, being initially placed at a maximum distance of about 3.5m from the building. They move towards the end of the pathway, where the evacuation test is considered to finish.

2.4. Variable parameters of the generic simulator for comparison purposes

The properties of *portals* and *servers* are the variable parameters for the setup of MassMotion, thus pursuing a sustainable and rapid configuration of the generic software for flood evacuation simulation. Thus, the following criteria for the setup configurations of *portals* and *servers* are considered in this work, as also resumed in Appendix B and as graphically shown by Figure 1 and Table 1:

1. *Entrance portals shape*. Two configurations are tested to represent the moment from building exit by pedestrians who try to start the evacuation together, because of group behaviors:

a. in the *rectangular* one, entrance *portals* have a dimension of 3x1m and are adjacent to the walls. The pedestrian density is about 3pp/m^2 in order to increase the interaction between them, starting the simulation closer to each other and lesser than 3.0m away from the unmovable obstacle;

b. in the *squared* one, where entrance *portals* have a dimension of 3x3m and are placed 1m away from the walls. The pedestrian density is about 1pp/m^2 to replicate the custom simulator starting setup.

2. *Servers number, positioning, and properties*. Servers are placed along the pathway (in the following, "first servers") and at the end of the *floor*, that is near the exit *portals* (in the following "second servers") to simulate the attraction of the pedestrians towards the buildings. Considering the *floor*'s length, each pedestrian's journey is aimed at using: 1 entrance *portal* at the beginning of the *floor*, 1 "first server" placed along the *floor*, 1 "second server" at the end of the *floor*, and finally 1 exit *portal*. The reference work distinguishes three main classes of distance from unmovable obstacles: 0 to 1m, 1 to 2m, 2 to 3m (Bernardini, Postacchini, et al., 2017). Therefore, three "first servers" per side of the *floor* are tested. An alternative configuration of only two "first servers" is also studied to increase the interaction between the pedestrians. In both cases, only one "second server" per side of the *floor* is tested to increase the attraction by the unmovable objects near the crossroads. These multiple setups are evaluated by placing servers in the middle (e.g. for the 0 to 1m class, 0.5m) or at the maximum value of each distance class (in the same example, 1m). Furthermore, the "first servers" position along the pathway is tested according to three configurations, according to a parametric approach. Tested positions are at *halfway*, at *a quarter*, and at *an eighth* of the pathway. These configurations allow investigating the impact of interferences between pedestrians at the passage points (i.e. servers), hence if behavioral uncertainties towards the unmovable obstacles exist. Finally, the probability that a pedestrian selects one of the "first servers" is assumed according to two configurations: *homogeneous*, if each element has the

same probability; *by-literature*, according to the real-world observations about the frequency for each class of distance from unmovable obstacles.

These criteria lead to obtaining 36 different setups, that are organized by grouping them by the entrance *portals* shape (R for rectangular; S for squared - in yellow in Figure 1) and the "first servers" position along the pathway (8 for position 1/8 of the path length; 4 for position 1/4 of the path length; 2 for position 1/2 of the path length - in magenta in Figure 1), as shown in Figure 1. Furthermore, each group of setups is also characterized by the probability a pedestrian can choose a *server* (H: homogeneous; L: by-literature), and the *servers'* number and position in respect to the wall (in orange in Figure 1), as resumed in Table 1.

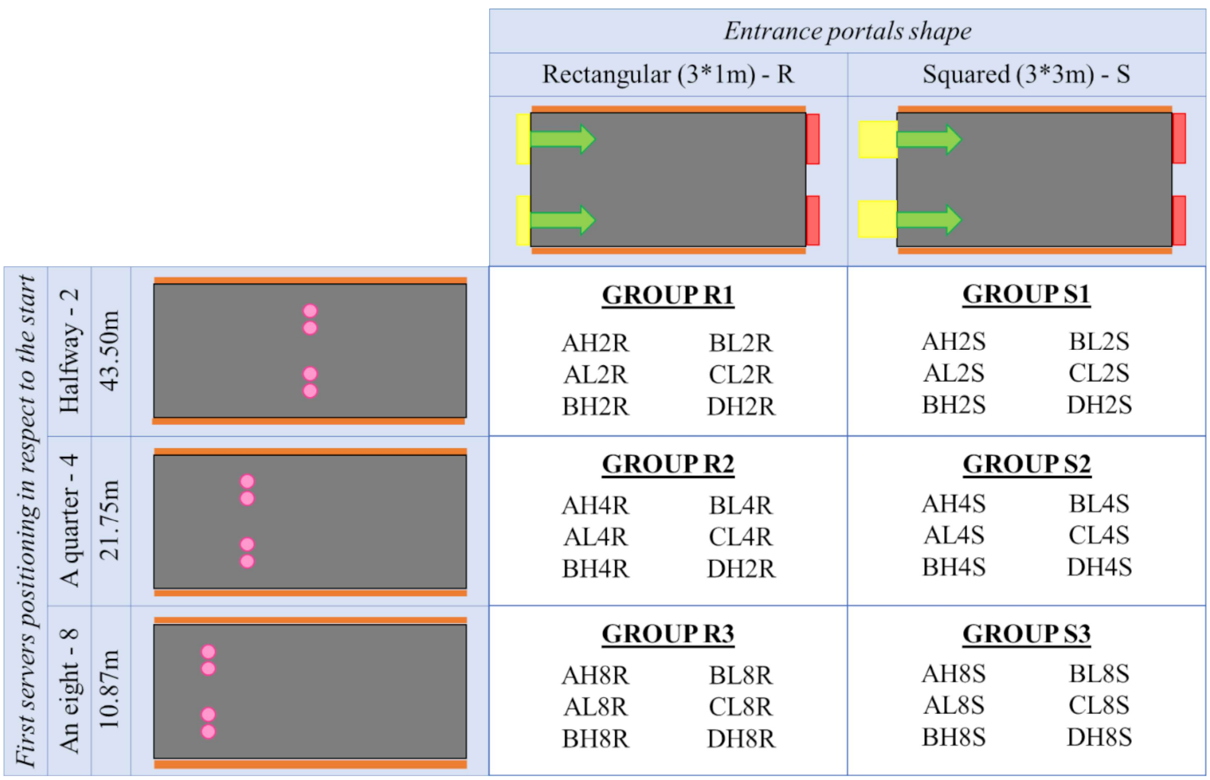

Figure 1: Setup groups organization depending on the entrance portals' shape (columns) and the "first servers" position along the pathway (rows). The setup code is composed of four characters: the number and position of the servers in respect to the wall (A-B-C-D) as in Table 1, the probability a pedestrian can choose a server (H-L), the

server position with respect to the start (2-4-8), and the shape of the entrance portal (R-S). Entrance portals are in yellow, exit portals in red, first servers in magenta, and buildings walls in orange.

Setup code	"First servers" features		"Second server" features	
	Number [-]	Distance from the wall [m]	Number [-]	Distance from the wall [m]
A	2	1; 2	1	1
B	2	0.5; 1.5	1	0.5
C	3	0.5; 1.5; 2.5	1	0.5
D	2	1; 2	1	0.5

Table 1: Setup code for the servers' position by considering their number and distance in respect of the side of the floor (i.e., the walls of the buildings).

2.5. Simulation outputs and comparison criteria

Simulations are repeated 10 times due to the probabilistic rules in motion simulation (Ronchi et al., 2013). Table 2 summarizes the simulations outputs from the generic and the custom software. They are selected in order to provide both a macroscopic (EC, t_{max}, W, and F) and a microscopic (D_w trends) description of the models, together with the necessity of comparison with real-world observations (D_w percentage distribution).

OUTPUT	DESCRIPTION
Graphical outputs	
Evacuation Curves EC	Evaluated as the percentage of arrived pedestrians [%] over the simulation time [s]. The average evacuation curve is considered for each tested condition.

D_w trends [m]	Distance between each pedestrian and the side of the building during the evacuation tracked over the pathway length. The outcoming curves describe how the attraction from unmovable obstacles affects the pedestrians' trajectory along the path, depending on the input setup. To elaborate these curves, D_w data are organized in quartiles. Data are grouped over 3m-long pathway steps, according to the distance threshold for repulsive phenomena in motion considered by FlooPEDS and based on previous works relating to the SFM
Numerical outputs	
Maximum evacuation time t_{max} [s]	The overall time during which the pedestrians remain in the outdoor BE.
Waiting time percentage W [%]	Calculated as the maximum waiting time t_w [s] (i.e., that is the time in which a pedestrian remains stationary at a *server*) normalized by the maximum evacuation time t_{max}. This parameter evaluates the impact of possible queuing phenomena simulated by the generic simulator at the *servers,* and considers how the effect of group dynamics can force pedestrians to spend time in non-movement activities because of simulator logics (in MassMotion, *servers* attract people towards the buildings but could represent deadlocks).
Evacuation flow F [pp/s]	Calculated as 5-to-95th percentiles of pedestrians to estimate the speediness of the evacuation process on a sample of 100 pedestrians (10 simulation repetitions of scenarios involving 10 pedestrians) to reduce the impact of outliers due to particular simulation aspects in crowd motion (Ronchi et al., 2013; Schadschneider et al., 2009), such as those related to starting positions less or more favorable, neighbors behaviors, deadlocks phenomena, etc.

D_w percentage distribution [%]	Percentage distribution of the distance between each pedestrian and the side of the building during the evacuation tracked over the pathway length, evaluated by considering the three literature-based main classes (Bernardini, Postacchini, et al., 2017): lower than 1m; from 1m to 2m; higher than 2m.

Table 2: List of parameters for the comparison between the generic and the custom simulator.

The comparison between the graphical outputs (i.e., *EC* and D_w trends) is performed according to previous works Key Performance Indicators (KPIs) resumed in Table 3 (D'Orazio et al., 2015; Ronchi et al., 2013). Results are discussed through KPIs mean and standard deviation values for each of the 6 setup groups identified in Figure 1, while extended results for all the 36 setups are reported in Supplementary Materials S2.

KPI	MEANING
Secant Cosine *SC* [-]	to measure the differences of shape between two curves, as their first derivative (for *SC* next to 1, the shapes of the curves can be considered similar)
Euclidean Relative Difference *ERD* [-]	to measure the overall agreement between two curves, as the norm of the difference between two vectors (for *ERD* next to 0, the curves can be considered close)
Euclidean Projection Coefficient *EPC* [-]	to measure the scale factor, which is the best possible fit between two curves (for EPC next to 1 the curves can be considered similar)
Difference between the graphic Areas	to investigate if underestimating/overestimating contingencies exist (positive values point out that predictions for the generic simulator are over those of the custom one

Under the Curves *DAUC* [%]	

Table 3: KPIs to perform the comparison between the graphical outputs (evacuation curves EC and D_w trends) and their meaning (D'Orazio et al., 2015; Ronchi et al., 2013).

Finally, the criteria for the comparison between the numerical outputs (i.e., t_{max}, *F*, *W*, and D_w percentage distribution) are resumed in Table 4. Quartile-based analyses are organized depending on the shape of the *portals* to describe general uncertainties for the whole set of considered input setups, then notable values are compared with custom software and real-world observations. Concerning the percentage distributions, differences due to the modelling logics at both microscopic and macroscopic levels are assessed to be compared with acceptability thresholds, which are up to about 10%-20% (Robin et al., 2009; Schadschneider et al., 2009; Shiwakoti et al., 2008).

OUTPUT	COMPARISON CRITERIA
t_{max} [s]	Quartile based analyses and comparison with custom software outputs
F [pp/s]	Quartile based analyses and comparison with custom software outputs
W [%]	Quartile based analyses
D_w percentage distributions [%]	Comparisons with custom software and real-world observations

Table 4: Numerical outputs comparison criteria: as the custom simulator does not consider deadlocks in the building attraction, W outputs are discussed independently to evaluate the impact of the queuing phenomena on the evacuation timing in the generic simulator.

3. Results

Results are organized comparing outputs of the generic and custom simulators (Sections 3.1 to 3.3), then the comparison is extended to real-world observations (Section 3.4). Finally, the generic simulator fittest setup is selected and discussed (Section 3.5).

3.1. Evacuation curves comparison

The evacuation curves graphical comparison is shown in Figure 2. Table 5Table 5: KPIs measuring differences between evacuation curves obtained from each setup tested on the generic simulator and the one obtained from the custom simulator. Results are shown in terms of mean and standard deviation values according to the grouping criteria shown in Figure 1. resumes the KPIs measuring the differences of the evacuation curves obtained from each setup tested on the generic simulator computed in respect to custom simulator results. Results are shown in terms of mean and standard deviation values according to the grouping criteria shown in Figure 1. Average results per group are provided.

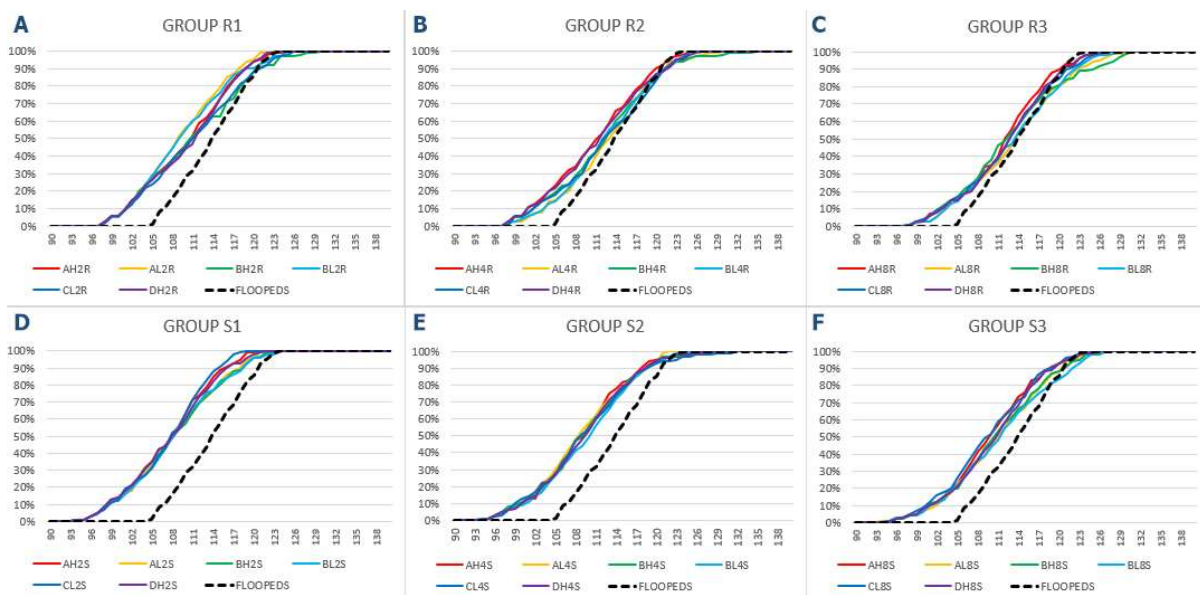

Figure 2: Comparison of the custom simulator evacuation curve (black dashed lined) and those of the generic simulator (straight lines). Generic simulator setups are grouped according to the criteria shown in Figure 1, that is considering the same entrance portals configuration, i.e., setup groups R1 to R3 are rectangular (panels A-B-C), S1 to S3 are squared (panels D-E-F).0-90s are omitted as no pedestrians complete the evacuation in this timespan.

Setup	*Values*	*SC*	*ERD*	*EPC*	*DAUC*
R1	**avg**	**0.777**	**0.170**	**1.038**	**13%**
	st. dev.	*0.031*	*0.025*	*0.016*	*2%*
R2	**Avg**	**0.849**	**0.102**	**1.008**	**7%**
	st. dev.	*0.035*	*0.024*	*0.011*	*2%*
R3	**avg**	**0.857**	**0.084**	**0.997**	**4%**
	st. dev.	*0.029*	*0.011*	*0.016*	*2%*
S1	**avg**	**0.710**	**0.260**	**1.073**	**22%**
	st. dev.	*0.021*	*0.016*	*0.009*	*2%*
S2	**avg**	**0.764**	**0.208**	**1.053**	**17%**
	st. dev.	*0.032*	*0.013*	*0.005*	*1%*
S3	**avg**	**0.822**	**0.157**	**1.035**	**12%**
	st. dev.	*0.028*	*0.021*	*0.013*	*2%*
OVERALL	**avg**	**0.796**	**0.164**	**1.034**	**13%**
	st. dev.	*0.060*	*0.063*	*0.028*	*6%*

Table 5: KPIs measuring differences between evacuation curves obtained from each setup tested on the generic simulator and the one obtained from the custom simulator. Results are shown in terms of mean and standard deviation values according to the grouping criteria shown in Figure 1.

The results highlight that, when the "first servers" position is closer to the entrance *portals*, that is for setup groups R3 and S3, the generic simulator outputs are closer to those of the custom simulator. In fact, in these cases, *SC* increases and *ERD* decreases. As expected, *EPC* seems non to be affected by the setup, as it tends to 1 in all the cases. In general, the generic simulator seems to underestimate the safety conditions of the pedestrian who arrives first by about 30% (see, for instance, Figure 2). Anyway, the *DAUC* always assumes positive values regardless of the proposed setup, meaning that the generic simulator slightly overestimates the entire evacuation process speed, as values range from 1 to 24%.

Considering the specificities of the setup groups, R2, R3, and S3 are the only ones with $SC>0.8$ and $ERD<0.2$, thus improving the similarities between the evacuation curves. These groups are characterized by smaller distances between the entrance *portals* and the *servers*. Slight differences can be noticed considering the number and positioning of the *servers* in respect to the side of the pathway, as the standard deviation values of all the KPIs point out, ranging between 0.01-0.03. On the other hand, when a pedestrian has the probability *by-literature* to select one of the "first servers", *SC*, *ERD,* and *DAUC* improve together with the curve shape similarity (see extended results for each setup in Supplementary Materials S1).

3.2. Comparison between D_w trend along the pathway

Table 6 resumes the analysis of the D_w trend according to the KPIs and considering the median distribution on a 3m resolution along the pathway. Results are grouped according to Figure 1 criteria, while simulation outputs for the 1st and 3rd quartile are available in Supplementary Materials S2. Average and standard deviation values per group are provided.

As for Section 3.1 results, setup groups characterized by smaller distances between the entrance *portals* and the *servers* seem to lead to more similar results in respect of the custom simulator, as shown by the median D_w trends in Figure 3. This result is mainly remarked by the *SC* values for groups R3, S2, and S3 ranging between 0.45-0.54, which is significantly higher if compared to other setup groups, thus implying that the *server* constraint should be placed closer to the start to effectively attract pedestrians near the unmovable obstacles (i.e., to reduce the curve subtended area). In this sense, such results seem to confirm those on the evacuation curve. However, the *SC* variability between the setups in the groups demonstrates some differences in D_w trends, as standard deviation values range from 0.07 to 0.12, while they are up to 0.20 considering the overall sample. Nevertheless, it is worth noticing that a limited correspondence between all the setups and the custom simulator outputs on D_w appears according to the other KPIs, as shown by Table 6 samples.

Setup	*Values*	*SC*	*ERD*	*EPC*	*DAUC*
R1	**avg**	**0.048**	**0.579**	**1.293**	**37%**
	st. dev.	*0.070*	*0.064*	*0.076*	*9%*
R2	**avg**	**0.316**	**0.448**	**1.203**	**27%**
	st. dev.	*0.073*	*0.062*	*0.082*	*10%*
R3	**avg**	**0.447**	**0.446**	**1.173**	**25%**
	st. dev.	*0.108*	*0.070*	*0.089*	*10%*
S1	**avg**	**0.170**	**0.510**	**1.278**	**34%**
	st. dev.	*0.096*	*0.060*	*0.067*	*8%*
S2	**avg**	**0.542**	**0.416**	**1.214**	**27%**
	st. dev.	*0.083*	*0.077*	*0.085*	*10%*
S3	**avg**	**0.506**	**0.409**	**1.166**	**23%**
	st. dev.	*0.121*	*0.074*	*0.093*	*11%*
OVERALL	**avg**	**0.338**	**0.468**	**1.221**	**29%**
	st. dev.	*0.203*	*0.090*	*0.096*	*11%*

Table 6: KPIs measuring differences between curves tracing the Dw trend for each setup tested on the generic simulator and the one obtained from the custom simulator (2nd quartile data). Results are shown in terms of mean and standard deviation values according to the grouping criteria shown in Figure 1. Extended results for each setup are in Supplementary Materials S3.

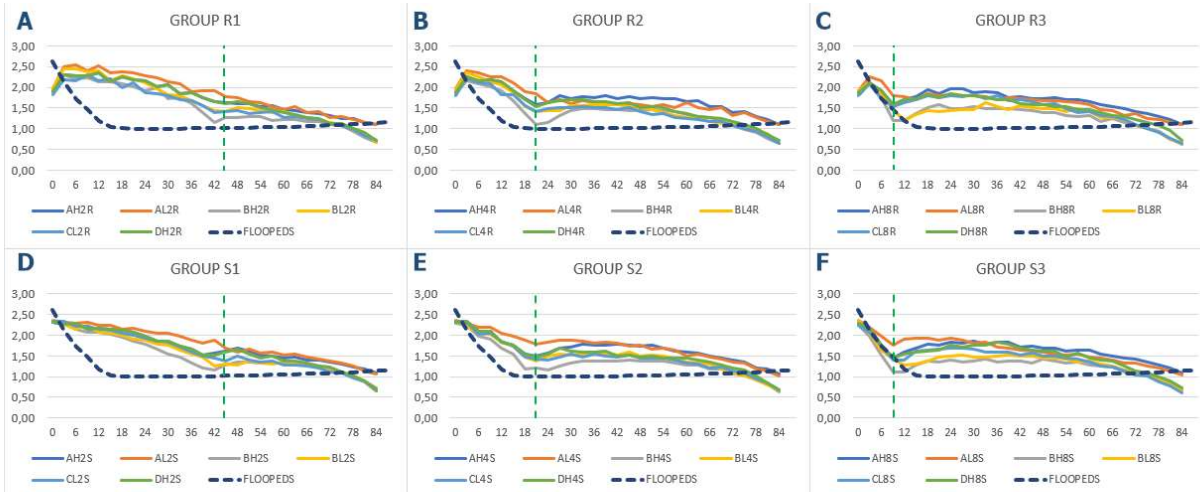

Figure 3: Comparison of 2nd quartile D_w trend for the custom simulator (blue dashed line) and those of the generic simulator (straight lines). Generic simulator setups are grouped according to the criteria shown in Figure 1, that is considering the same entrance portals configuration, i.e., setup groups R1 to R3 are rectangular (panels A-B-C), S1 to S3 are squared (panels D-E-F). The green dashed line indicates the position of the "first servers" along the pathway.

3.3. Quartile analysis of trends in pedestrians' evacuation timing

Overall outcomes about the maximum evacuation time t_{max} (Figure 4) show similar results between the two simulators (1s difference between the custom simulator and the generic one mean value). Concerning the distinction by setup, the percentage differences range between -4% and 4% considering all the setup tested but the outliers (blue box). Differences between squared and rectangular portals seem to be negligible (<5%), even if groups 'R' (i.e., rectangular *entrance portals*) register slightly higher t_{max} values. This result seems to be affected by repulsion forces between pedestrians in those entrance areas, and their effects are increased by the high-density conditions (about 3 pp/m^2) in the rectangular portals. As a consequence, these conditions imply the pedestrians' trajectories are farther from the pathway sides while they are approaching the "first servers" (as shown in Figure 3).

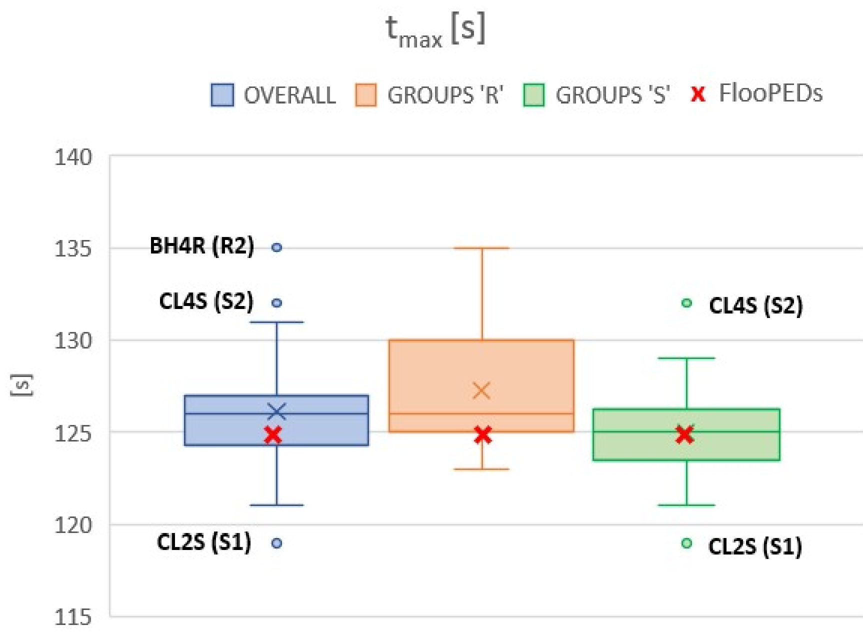

Figure 4: Comparison between the maximum evacuation time t_{max} of the custom simulator (red cross) and the generic simulator distinguishing overall (blue box) and groups data (orange and green boxes). Outlier setups are marked as follows: "Setup name (Group name)". Extended results for each setup are in Supplementary Materials S4.

In general, a queue formation trend can be noticed because all pedestrians start at the same time and place, and they are "forced" to pass by the *server*. Some pedestrians could be forced to stop the evacuation for some time. Thus, regarding the maximum waiting time percentage *W*, the comparison between all the setups in Figure 5 shows how pedestrians behave similarly regardless of the shape of the *entrance portals* and the *servers'* features (i.e., their position and number), as differences between maximum and minimum values are only of about 7% (blue box). Anyway, absolute waiting times are in the range between 5-15s, which is reasonable for flood outdoor evacuations where circumstances like social attachment, group phenomena, and difficulties in motion and stability can force pedestrians to stop (Bernardini et al., 2019).

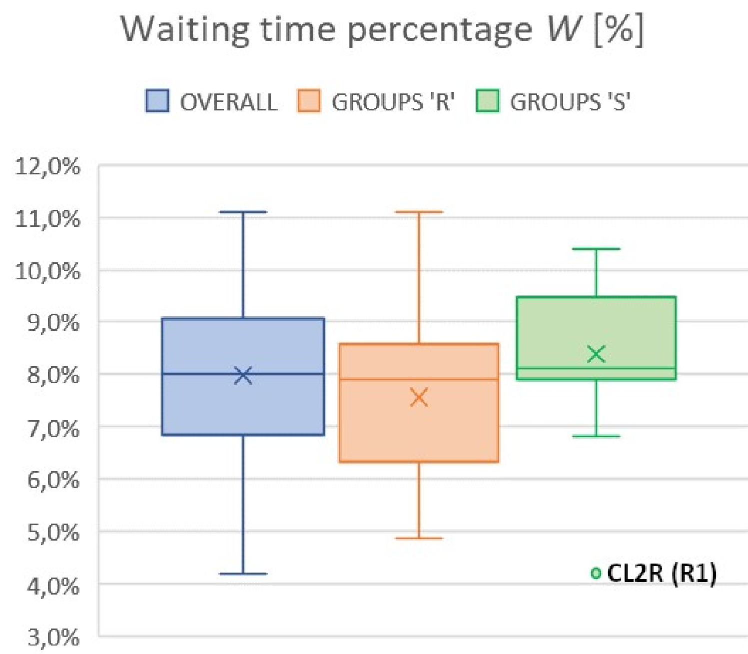

Figure 5: boxplot representation of the maximum waiting time percentage W, distinguishing overall (blue box) and groups data (orange and green boxes. Outlier setups are marked as follows: "Setup name (Group name)".

Finally, Figure 6 shows how group phenomena seem to have a greater impact in the generic software than in the custom simulator regardless of the setup tested. Indeed, the evacuation flows F are 30% smaller considering the mean values of all the setup groups, and percentage differences between setups are <5% (excluding the outliers highlighted in Figure 6). Such phenomena could be linked to the aforementioned "forced" passage by the servers

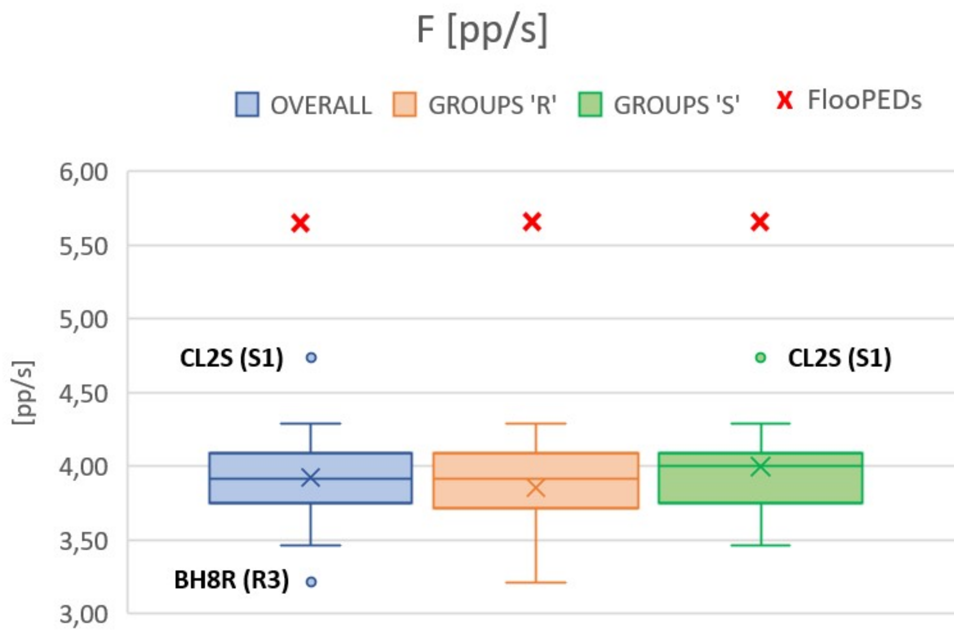

Figure 6: Comparison between the evacuation flow F values of the custom simulator (red cross) and of the generic simulator distinguishing overall (blue box) and groups data (orange and green boxes). Outlier setups are marked as follows: "Setup name (Group name)". Extended results for each setup are in Supplementary Materials S5.

3.4. Comparison with real-world observations

The positioning of "attraction" objects (i.e., the *servers*) ensures the representation of attraction phenomena towards unmovable obstacles (i.e., the *floor* edges). According to Section 2.4, *homogeneous* or *by-literature* setups are tested, thus representing different probabilities that a pedestrian can choose one of the "first servers".

Table 7 compares the D_w percentage distribution of the distance between pedestrians and unmovable obstacles from the generic simulator with those obtained, respectively, from the real-world observations (as a reference for the comparison (Bernardini, Postacchini, et al., 2017)), and the custom simulator. Results show non-significant differences between the setup groups, as the standard deviations range, in general, between 1-5%. On the other hand, the comparison with the custom simulator and the real-world observations from previous literature works shows more significant differences. In particular, concerning the $1<D_w\leq 2$m class, these differences are essentially due to the

repulsive forces between pedestrians in the same group, which induce lower frequency in this class of distance (negative differences). On the other hand, D_w>2m is more frequent in the generic simulator compared to what is observed in the real world and the custom simulator (positive differences). Thus, from the behavioral modelling point of view, the generic simulator conservatively overestimates the risk condition during the evacuation, as pedestrians will travel wider trajectories in their route to safety, hence facing longer exposition to risk through longer evacuation paths. In addition to this, from a hydrodynamic point of view, the overestimation of D_w also lead to a decrement of the pedestrians' speed and problems of instability as the streets in general behave like open channels and the water speed increases moving away from the edges (Chow, 1959) (compare with Equation 1). However, it is worth noting that we actually consider stationary conditions in this first, simple testing scenario, which implies having the same evacuation speed v_i on each point of the floor regardless of the pedestrians' distance from the side of the buildings.

	Pedestrians' frequency percentage distribution and variability [%]			
	Dw≤1m [%]	***1<Dw≤2m [%]***	***Dw>2m [%]***	
Real-world observations from literature	29	50	21	
Custom simulator	23	66	11	
Generic simulator setup				
R1	37 (L: +8; C: +14)	29 (L: -21; C: -37)	34 (L: +13; C: +23)	Avg
	4	1	4	Dev. St.
R2	38 (L: +9; C: +15)	31 (L: -19; C: -35)	31 (L: +10; C: +20)	Avg
	4	2	5	Dev. St.
R3	37 (L: +8; C: +14)	33 (L: -17; C: -33)	30 (L: +9; C: +19)	Avg
	4	2	4	Dev. St.
S1	36 (L: +7; C: +13)	29 (L: -21; C: -37)	35 (L: +14: C: +24)	Avg
	4	1	4	Dev. St.
S2	36 (L: +7; C: +13)	32 (L: -18; C: -34)	32 (L: +11; C: +21)	Avg
	4	1	4	Dev. St.
S3	36 (L: +7; C: +13)	34 (L: -16; C: -32)	30 (L: +9; C: +19)	Avg
	5	2	4	Dev. St.
OVERALL	37 (L: +8; C: +14)	31 (L: -19; C: -35)	32 (L: +11; C: +21)	Avg
	4	2	5	Dev. St.

Table 7: *Pedestrians frequency percentage distribution and variability for each distance class: comparison of the setup of the generic simulator (grouped according to the criteria shown in Figure 1) with real-world observations from literature works (L)* (Bernardini, Postacchini, et al., 2017) *and the custom simulator data (C). Avg refers to average*

data, Dev. St. refers to the related standard deviation of the sample. Extended results for each setup are in Supplementary Materials S6.

3.5. Best setup discussion

The organization of the results in setup groups allowed finding a key element for the modelling of the simulation environment, that is the position of the *servers*. Indeed, the positioning of these attraction points closer to the *entrance portals* seems to be the most influential option which allows having graphical outputs as similar as possible to those of the custom simulator (i.e., evacuation curves in Figure 2 and D_w trends in Figure 3, groups R3 and S3). Furthermore, this positioning also helps to obtain simulations consistent with real-world observations, as groups R3 and S3 are the ones with the closer distribution to real-world observations in the $1<D_w\leq 2$m class (Table 7).

However, between all the setups tested, the BL8S (group S3) is the one that produced the closest results to the custom simulator, and is characterized by the following features that support the similarities with the custom simulator:

- The condition of the *squared entrance portals*, in which pedestrians are generated with a density of about 1pp/m^2, is similar to those of the custom simulator. The initial effect of the repulsive force between pedestrians seems to be mitigated because of their mutual distance, which is preserved along the pathway. Meanwhile, in the other configuration, the density is 3 times higher, so that pedestrians spread out at the very beginning of the pathway;
- *Two "first servers"* are positioned at 1/8 of the pathway length (i.e., about 10m from the start). This condition allows increasing the attraction towards unmovable obstacles and the interaction between the pedestrians. Considering the distance from the side of the pathway, the "first servers" are placed in the middle of each class of distance (i.e., *servers* at 0.5m and 1.5m from the wall), with a *by-literature* probability distribution for pedestrians to select one of them. This element of the setup seems to reduce the MassMotion trend in simulating higher

pedestrian-unmovable obstacles distances. Anyway, having *servers* extremely close to the start of the pathway could represent a problem for what it concerns queue phenomena, especially with very large groups of pedestrians.

Figure 7 shows the evacuation curves and the D_w trends obtained from the proposed setup (red solid lines) and the custom simulator (black dashed lines). According to the results on KPIs introduced in Section 2.52.53.4, the evacuation curves are similar in shape and size (SC=0.78, EPC=1.01), close to each other (ERD=0.13), and without significant differences in underestimating/overestimating contingencies (DAUC=9%). Anyway, it is worthy of notice that the generic simulator seems to speed up the evacuation process for the first arrived pedestrians, which can be considered as free to move in the environment and to pass by the server with a reduction of group interactions. In this sense, the custom simulator better points out the group attraction phenomena, by reducing the time gap between the first and the last arrived pedestrians. However, in view of the above, considering such risk conditions in terms of the pedestrians' density and practicability conditions (i.e., pedestrians still manage to move in the floodwater without experiencing instability problems), the two simulators produce comparable results concerning macroscopic aspects like the over-time progression of the evacuation process (i.e., evacuation curves *EC*, flow *F*, and maximum evacuation time t_{max}).

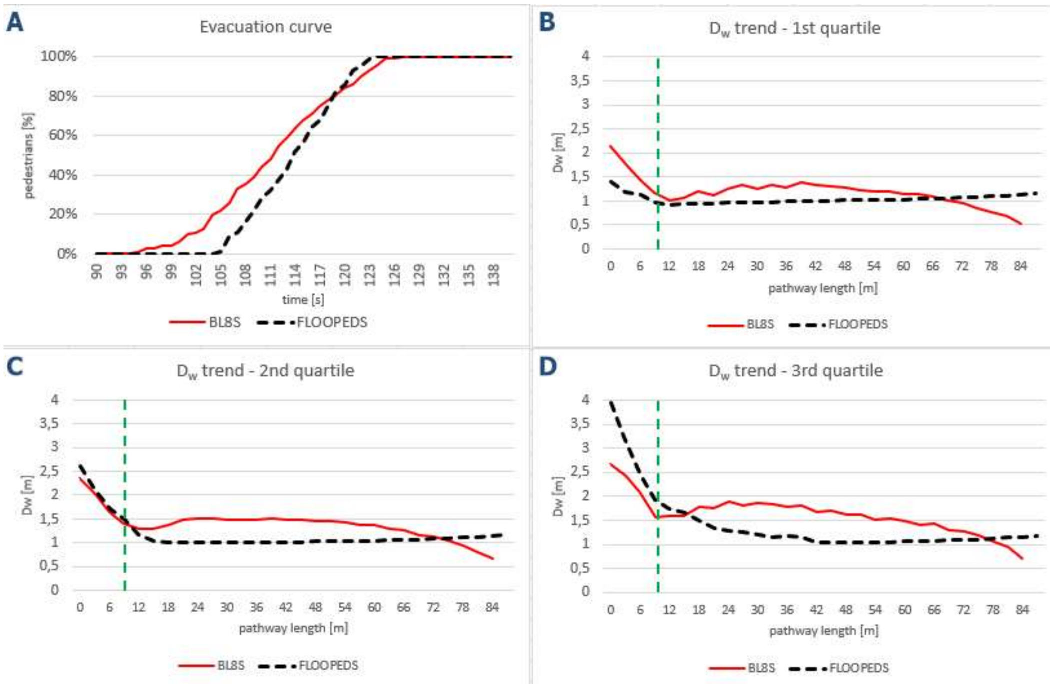

Figure 7: Comparison between the evacuation curves (panel A) and the D_w trends (panels B-C-D) obtained from the BL8S setup of the generic simulator (red solid lines) and the custom simulator (black dashed lines). The green dashed line indicates the "first servers" position along the pathway. The evacuation curves comparison considers the range between 90-140s, which from the arrival of the first pedestrian to the exit of the last one.

On the other hand, from a microscopic point of view, differences emerge in pedestrians' trajectories, as the D_w outcomes point out. In particular, the generic simulator BL8S setup seems to overestimate the pedestrians' risk if considering their trajectories, because the setup and the model force them to travel along larger trajectories towards the evacuation target. This implies higher exposition for pedestrians to the floodwaters (Chow, 1959), especially after the attraction points effect (i.e., the "first server") as shown in Figure 7. Table 8 summarizes the KPIs values concerning the D_w trends comparison, showing differences in the curves' shape and overall agreement. However, considering the probability distributions in class distances (Table 9), the generic simulator setup finds good agreement with the real-world observations (differences <15%), meaning that the general trends can be considered as preliminary acceptable for simulation purposes (Robin et al., 2009; Schadschneider et al., 2009; Shiwakoti et al., 2008).

	SC	***ERD***	***EPC***	***DAUC***
1st quartile	0.53	0.36	1.10	10%
2nd quartile	0.71	0.33	1.09	14%
3rd quartile	0.65	0.35	0.99	11%

Table 8: KPIs measuring differences between curves tracing the Dw trend of the generic simulator best setup (BL8S) and the custom simulator (quartile analysis).

	Dw≤1m [%]	***1<Dw≤2m [%]***	***Dw>2m [%]***
Real-world observations from literature	29	50	21
Custom simulator	*23*	*66*	*11*
BL8S setup	*39*	*37*	*25*

Table 9: Pedestrians' frequency percentage distribution for each distance class: comparison of the generic simulator best setup (BL8S) with the literature distributions (Bernardini, Postacchini, et al., 2017) *and the custom simulator distributions. Percentage differences between literature (L) and custom software (C) data are pointed out in brackets.*

Finally, Table 10 shows the pedestrians' evacuation timing data concerning: (a) the maximum evacuation time t_{max}, which is almost identical between the two analyzed software, thus confirming non-particular underestimating/overestimating safety contingencies, (b) the waiting time percentage W, and (c) the evacuation flow F, whose values are by the way in line with the generic simulator overall trend.

	t_{max} [s]	W [%]	F [pp/s]
Custom simulator	125	-	5.63
Generic simulator (median)	126	8%	3.91

BL8S setup	***127 (C: 2%; G: 1%)***	***10% (C: -; G: 2%)***	***3.75 (C: -33%; G: -4%)***

Table 10: Comparison of the maximum evacuation time t_{max}, the waiting time percentage W, and the evacuation flow F of the generic simulator best setup (BL8S): percentage differences between the custom simulator (C) and the generic software median data (G) are pointed out into brackets.

4. Conclusions

The present work is a very first attempt to implement an outdoor flood evacuation model in a generic evacuation simulation software (MassMotion) to ease and speed up the risk assessment analyses by using a quick no-code modification approach. Functions and features already included in the generic software are used to this end. Thus, different setups are tested to describe the pedestrians-floodwaters interactions during a flood evacuation in a simple typological scenario like a straight and flat street. As a benchmark, a previously developed and tested custom flood evacuation simulator is selected, that is FlooPEDs (Flooding Pedestrians' Evacuation Dynamics Simulator). Stationary flood conditions and compact groups of 10 pedestrians are considered in the comparison, which is consistent with basic conditions in outdoor BE evacuation after the peak of the event, but sufficiently detailed to represent a valid preliminary test. Simulation outputs are organized to identify the best setup, which is the one that produces the closest outcomes to the ones of the custom simulator.

Considering the best setup, the comparison of the results shows slight differences between the two software. Indeed, from a macroscopic point of view, the generic simulator manages to represent the main effects of the flood evacuation as proved by outcomes in terms of evacuation timing. On the other hand, considering microscopic aspects such as the pedestrian trajectories along the pathway, the best setup shows good agreement with the real-world observations, while marked differences with respect to the custom simulator still exist. In particular, it is worth noticing that the generic simulator seems to overestimate the risk for pedestrians by computing higher distances from unmovable objects, thus implying lower evacuation speed and higher exposure to the water flow for pedestrians.

Anyway, additional tests on more complex scenarios, real-world contexts, and pedestrians' features (e.g. investigating larger groups of pedestrians and/or with different physical and social features) are still encouraged, assuming the best setup of this work. To this end, the same proposed setup methodology and comparison criteria could be adopted and support researchers in such preliminary validation and verification tasks.

Moreover, next research steps should also move towards modifications to the generic software code to include SFM-related interactions to overcome current setup-based simulator limitations in describing the outdoor evacuation behaviors in complex BEs (i.e., with the effective implementation of unmovable objects like trees, walls, fences, that can have an attractive effect on the pedestrians). Similarly, to overcome the use of (pseudo-)stationary conditions in floodwaters, the variations in floodwaters levels to represent hydrodynamics conditions could be managed by directly connecting input data from external hydrodynamic simulators, thus adapting flood inputs affecting the pedestrians' motion and decision-making.

Anyway, the proposed tool could be used by low-trained technicians and Local Authorities to preliminary assess evacuation risks in BEs, to propose risk-mitigation strategies (i.e. architectural layout modifications, micro-scale re-thinking of built spaces, direct support to pedestrians by also using wayfinding and alert systems, management actions by rescuers, "invacuation" strategies) as well as to increase the pedestrian safety to flood in both indoor and outdoor BEs, characterized by similar scenario conditions (e.g. wide spaces in public buildings or undergrounds), in both existing and new ones.

5. References

Ashley, S. T., & Ashley, W. S. (2008). Flood fatalities in the United States. *Journal of Applied Meteorology and Climatology*. https://doi.org/10.1175/2007JAMC1611.1

Bazin, P.-H., Mignot, E., & Paquier, A. (2017). Computing flooding of crossroads with obstacles using a 2D numerical model. *Journal of Hydraulic Research*, *55*(1), 72–84. https://doi.org/10.1080/00221686.2016.1217947

Beretta, R., Ravazzani, G., Maiorano, C., & Mancini, M. (2018). Simulating the influence of buildings on flood inundation in Urban areas. *Geosciences (Switzerland)*. https://doi.org/10.3390/geosciences8020077

Bernardini, G., Camilli, S., Quagliarini, E., & D'Orazio, M. (2017). Flooding risk in existing urban environment: from human behavioral patterns to a microscopic simulation model. *Energy Procedia*, *134*, 131–140. https://doi.org/10.1016/j.egypro.2017.09.549

Bernardini, G., Finizio, F., Postacchini, M., & Quagliarini, E. (2021). Assessing the flood risk to evacuees in outdoor built environments and relative risk reduction strategies. *International Journal of Disaster Risk Reduction*, *64*, 102493. https://doi.org/10.1016/j.ijdrr.2021.102493

Bernardini, G., Postacchini, M., Quagliarini, E., Brocchini, M., Cianca, C., & D'Orazio, M. (2017). A preliminary combined simulation tool for the risk assessment of pedestrians' flood-induced evacuation. *Environmental Modelling and Software*. https://doi.org/10.1016/j.envsoft.2017.06.007

Bernardini, G., Quagliarini, E., & D'Orazio, M. (2019). Investigating Exposure in Historical Scenarios: How People Behave in Fires, Earthquakes and Floods. In *RILEM Bookseries*. https://doi.org/10.1007/978-3-319-99441-3_123

Bodoque, J. M., Amérigo, M., Díez-Herrero, A., García, J. A., Cortés, B., Ballesteros-Cánovas, J. A., & Olcina, J. (2016). Improvement of resilience of urban areas by integrating social perception in flash-flood risk management. *Journal of Hydrology*.

https://doi.org/10.1016/j.jhydrol.2016.02.005

Bosina, E., & Weidmann, U. (2017). Estimating pedestrian speed using aggregated literature data. *Physica A: Statistical Mechanics and Its Applications*, *468*, 1–29. https://doi.org/10.1016/j.physa.2016.09.044

Chang, H., Pallathadka, A., Sauer, J., Grimm, N. B., Zimmerman, R., Cheng, C., Iwaniec, D. M., Kim, Y., Lloyd, R., McPhearson, T., Rosenzweig, B., Troxler, T., Welty, C., Brenner, R., & Herreros-Cantis, P. (2021). Assessment of urban flood vulnerability using the social-ecological-technological systems framework in six US cities. *Sustainable Cities and Society*, *68*. https://doi.org/10.1016/j.scs.2021.102786

Chow, V. T. (1959). Open-Channel Hydraulics. Ven Te Chow. McGraw-Hill, New York, 1959. xviii + 680 pp. Illus. $17. In *Science*.

Cox, R. J., & Shand, T.D.Blacka, M. J. (2010). Australian Rainfall & Runoff revision project 10: Appropriate safety criteria for people. In *Engineers Australia*. https://doi.org/10.1038/103447b0

D'Orazio, M., Longhi, S., Olivetti, P., & Bernardini, G. (2015). Design and experimental evaluation of an interactive system for pre-movement time reduction in case of fire. *Automation in Construction*, *52*, 16–28. https://doi.org/10.1016/j.autcon.2015.02.015

da Silva, L. B. L., Alencar, M. H., & de Almeida, A. T. (2022). A novel spatiotemporal multi-attribute method for assessing flood risks in urban spaces under climate change and demographic scenarios. *Sustainable Cities and Society*, *76*(July 2021), 103501. https://doi.org/10.1016/j.scs.2021.103501

Dai, Q., Zhu, X., Zhuo, L., Han, D., Liu, Z., & Zhang, S. (2020). A hazard-human coupled model (HazardCM) to assess city dynamic exposure to rainfall-triggered natural hazards. *Environmental Modelling & Software*, *127*(May 2019), 104684. https://doi.org/10.1016/j.envsoft.2020.104684

Dias, C., Rahman, N. A., & Zaiter, A. (2021). Evacuation under flooded conditions: Experimental investigation of the influence of water depth on walking behaviors. *International Journal of Disaster Risk Reduction*, *58*(November 2020), 102192. https://doi.org/10.1016/j.ijdrr.2021.102192

Domingo, D., Palka, G., & Hersperger, A. M. (2021). Effect of zoning plans on urban land-use change: A multi-scenario simulation for supporting sustainable urban growth. *Sustainable Cities and Society*, *69*. https://doi.org/10.1016/j.scs.2021.102833

Dong, S., Yu, T., Farahmand, H., & Mostafavi, A. (2020). Probabilistic modeling of cascading failure risk in interdependent channel and road networks in urban flooding. *Sustainable Cities and Society*, *62*. https://doi.org/10.1016/j.scs.2020.102398

European Commission. (2017). Overview of natural and man-made disaster risks in the European Union may face. In *Commission Staff Working Document*. https://doi.org/doi:10.2795/861482

Fan, Q., Tian, Z., & Wang, W. (2018). Study on Risk Assessment and Early Warning of Flood-Affected Areas when a Dam Break Occurs in a Mountain River. *Water*, *10*(10), 1369. https://doi.org/10.3390/w10101369

French, E. L., Birchall, S. J., Landman, K., & Brown, R. D. (2019). Designing public open space to support seismic resilience: A systematic review. *International Journal of Disaster Risk Reduction*, *34*, 1–10. https://doi.org/10.1016/j.ijdrr.2018.11.001

Fruin, J. J. (1971). Pedestrian planning and design. In *Metropolitan Association of Urban Designers and Environmental planners Inc*. Metropolitan Association of Urban Designers and Environmental Planners.

Gandini, A., Garmendia, L., Prieto, I., Álvarez, I., & San-José, J. T. (2020). A holistic and multi-stakeholder methodology for vulnerability assessment of cities to flooding and extreme precipitation events. *Sustainable Cities and Society*. https://doi.org/10.1016/j.scs.2020.102437

Gandini, A., Quesada, L., Prieto, I., & Garmendia, L. (2021). Climate change risk assessment: A holistic multi-stakeholder methodology for the sustainable development of cities. *Sustainable Cities and Society*, *65*. https://doi.org/10.1016/j.scs.2020.102641

Gu, D. (2019). *Exposure and vulnerability to natural disasters for world's cities. United Nations, Department of Economics and Social Affairs, Population Division, Technical Paper No. 4*. (Population Division, Technical Paper No. 4., Issue Technical Paper No. 4.). https://www.un.org/en/development/desa/population/publications/pdf/technical/TP2019-4.pdf

Han, Y., & Mozumder, P. (2022). Risk-based flood adaptation assessment for large-scale buildings in coastal cities using cloud computing. *Sustainable Cities and Society*, *76*. https://doi.org/10.1016/j.scs.2021.103415

Helbing, D., Farkas, I., & Vicsek, T. (2000). Simulating dynamical features of escape panic. *Nature*, *407*(6803), 487–490. https://doi.org/10.1038/35035023

Jamrussri, S., & Toda, Y. (2018). Available Flood Evacuation Time for High-Risk Areas in the Middle Reach of Chao Phraya River Basin. *Water*, *10*(12), 1871. https://doi.org/10.3390/w10121871

Jebrane, A., Argoul, P., Hakim, A., & El Rhabi, M. (2019). Estimating contact forces and pressure in a dense crowd: Microscopic and macroscopic models. *Applied Mathematical Modelling*, *74*, 409–421. https://doi.org/10.1016/j.apm.2019.04.062

Jia, X., Morel, G., Martell-Flore, H., Hissel, F., & Batoz, J.-L. (2016). Fuzzy logic based decision support for mass evacuations of cities prone to coastal or river floods. *Environmental Modelling & Software*, *85*, 1–10. https://doi.org/10.1016/j.envsoft.2016.07.018

Kim, J., Park, J., Kim, K., & Kim, M. (2021). RnR-SMART: Resilient smart city evacuation plan based on road network reconfiguration in outbreak response. *Sustainable Cities and Society*, *75*, 103386. https://doi.org/10.1016/j.scs.2021.103386

Kolen, B., & van Gelder, P. H. A. J. M. (2018). Risk-Based Decision-Making for Evacuation in Case of Imminent Threat of Flooding. *Water*, *10*(10), 1429. https://doi.org/10.3390/w10101429

Lakoba, T. I., Kaup, D. J., & Finkelstein, N. M. (2005). Modifications of the Helbing-Molnar-Farkas-Vicsek Social Force Model for Pedestrian Evolution. *Simulation*, *81*(5), 339–352.

https://doi.org/10.1177/0037549705052772

Lee, H.-K., Hong, W.-H., & Lee, Y.-H. (2019). Experimental study on the influence of water depth on the evacuation speed of elderly people in flood conditions. *International Journal of Disaster Risk Reduction*, *39*, 101198. https://doi.org/10.1016/j.ijdrr.2019.101198

Li, Y., Hu, B., Zhang, D., Gong, J., Song, Y., & Sun, J. (2019). Flood evacuation simulations using cellular automata and multiagent systems -a human-environment relationship perspective. *International Journal of Geographical Information Science*, *33*(11), 2241–2258. https://doi.org/10.1080/13658816.2019.1622015

Lumbroso, D., & Davison, M. (2018). Use of an agent-based model and Monte Carlo analysis to estimate the effectiveness of emergency management interventions to reduce loss of life during extreme floods. *Journal of Flood Risk Management*, *11*, S419–S433. https://doi.org/10.1111/jfr3.12230

MassMotion Guide. (2020). *MassMotion Guide*.

Matsuo, K., Natainia, L., & Yamada, F. (2011). Flood and Evacuation Simulations for Urban Flooding. *5th International Conference on Flood Management*, 391–398.

Mignot, E., Li, X., & Dewals, B. (2019). Experimental modelling of urban flooding: A review. *Journal of Hydrology*, *568*, 334–342. https://doi.org/10.1016/j.jhydrol.2018.11.001

Najafi, M. R., Zhang, Y., & Martyn, N. (2021). A flood risk assessment framework for interdependent infrastructure systems in coastal environments. *Sustainable Cities and Society*, *64*. https://doi.org/10.1016/j.scs.2020.102516

Opper, S., Cinque, P., & Davies, B. (2010). *Timeline modelling of flood evacuation operations*. *3*, 175–187. https://doi.org/10.1016/j.proeng.2010.07.017

Paquier, A., Mignot, E., & Bazin, P.-H. (2015). From Hydraulic Modelling to Urban Flood Risk. *Procedia Engineering*, *115*, 37–44. https://doi.org/10.1016/j.proeng.2015.07.352

Piyumi, M. M. M., Abenayake, C., Jayasinghe, A., & Wijegunarathna, E. (2021). Urban Flood Modeling Application: Assess the Effectiveness of Building Regulation in Coping with Urban

Flooding Under Precipitation Uncertainty. *Sustainable Cities and Society*, *75*. https://doi.org/10.1016/j.scs.2021.103294

Puchol-Salort, P., O'Keeffe, J., van Reeuwijk, M., & Mijic, A. (2021). An urban planning sustainability framework: Systems approach to blue green urban design. *Sustainable Cities and Society*, *66*, 102677. https://doi.org/10.1016/j.scs.2020.102677

Rezende, O. M., Miranda, F. M., Haddad, A. N., & Miguez, M. G. (2019). *A Framework to Evaluate Urban Flood Resilience of Design Alternatives for Flood Defence Considering Future Adverse Scenarios*.

Robin, T., Antonini, G., Bierlaire, M., & Cruz, J. (2009). Specification, estimation and validation of a pedestrian walking behavior model. *Transportation Research Part B: Methodological*. https://doi.org/10.1016/j.trb.2008.06.010

Ronchi, E. (2020). Developing and validating evacuation models for fire safety engineering. *Fire Safety Journal*, 103020. https://doi.org/10.1016/j.firesaf.2020.103020

Ronchi, E., Kuligowski, E. D., Reneke, P. A., Peacock, R. D., & Nilsson, D. (2013). The Process of Verification and Validation of Building Fire Evacuation Models. *NIST Technical Note*, *1822*.

Samany, N. N., Sheybani, M., & Zlatanova, S. (2021). Detection of safe areas in flood as emergency evacuation stations using modified particle swarm optimization with local search. *Applied Soft Computing*, *111*, 107681. https://doi.org/10.1016/j.asoc.2021.107681

Schadschneider, A., Klingsch, W., Klüpfel, H., Kretz, T., Rogsch, C., & Seyfried, A. (2009). Evacuation Dynamics: Empirical Results, Modeling and Applications. In Meyers R. (Ed.), *Encyclopedia of Complexity and Systems Science* (pp. 3142-3176 LA-English). Springer New York. https://doi.org/10.1007/978-0-387-30440-3_187

Shi, L., Xie, Q., Cheng, X., Chen, L., Zhou, Y., & Zhang, R. (2009). Developing a database for emergency evacuation model. *Building and Environment*, *44*(8), 1724–1729. https://doi.org/10.1016/j.buildenv.2008.11.008

Shirvani, M., & Kesserwani, G. (2021). Flood–pedestrian simulator for modelling human response dynamics during flood-induced evacuation: Hillsborough stadium case study. *Natural Hazards and Earth System Sciences*, *21*, 3175–3198. https://doi.org/10.5194/nhess-21-3175-2021

Shirvani, M., Kesserwani, G., & Richmond, P. (2020). Agent-based modelling of pedestrian responses during flood emergency: mobility behavioural rules and implications for flood risk analysis. *Journal of Hydroinformatics*, *22*(5), 1078–1092. https://doi.org/10.2166/hydro.2020.031

Shiwakoti, N., Sarvi, M., & Rose, G. (2008). *Modelling pedestrian behaviour under emergency conditions – State-of-the-art and future directions*. 457–473.

Soares-Frazão, S., Lhomme, J., Guinot, V., & Zech, Y. (2008). Two-dimensional shallow-water model with porosity for urban flood modelling. *Journal of Hydraulic Research*. https://doi.org/10.1080/00221686.2008.9521842

Takagi, H., Li, S., de Leon, M., Esteban, M., Mikami, T., Matsumaru, R., Shibayama, T., & Nakamura, R. (2016). Storm surge and evacuation in urban areas during the peak of a storm. *Coastal Engineering*, *108*, 1–9. https://doi.org/10.1016/j.coastaleng.2015.11.002

Wan Mohtar, W. H. M., Abdullah, J., Abdul Maulud, K. N., & Muhammad, N. S. (2020). Urban flash flood index based on historical rainfall events. *Sustainable Cities and Society*, *56*. https://doi.org/10.1016/j.scs.2020.102088

Young, A. F., & Jorge Papini, J. A. (2020). How can scenarios on flood disaster risk support urban response? A case study in Campinas Metropolitan Area (São Paulo, Brazil). *Sustainable Cities and Society*, *61*, 102253. https://doi.org/10.1016/j.scs.2020.102253

Zhuo, L., & Han, D. (2020). Agent-based modelling and flood risk management: A compendious literature review. *Journal of Hydrology*, *591*, 125600. https://doi.org/10.1016/j.jhydrol.2020.125600

6. Appendix A

In this section, we provide the specific software configuration terms, underlining MassMotion option in italics, and in square brackets, where needed. Three main elements compose the MassMotion testing scenario (MassMotion Guide, 2020): (1) the *floor*, simulating the linear pathway where *agents* (i.e. pedestrians) move; (2) the *portals*, representing both the entrances into the simulation and the *agents'* destinations; and (3) the *servers*, used in this work to reproduce the attraction of the *agents* (i.e. pedestrians) towards unmovable obstacles (i.e. buildings).

Entrance only and *destination portals* (respectively, where *agents* enter and exit the simulation *floor*) are placed close to the later *floor* limit, to reproduce the ideal maximum distance among pedestrians and buildings according to the considered real-world observations (Bernardini, Postacchini, et al., 2017). An *entrance only portal* (whose dimensions depend on the setup tested) and a *destination portal* are placed at each *floor* side.

The *servers* are introduced to increase the attraction behavior towards unmovable obstacles, that are the pathways sides. The start points of the *servers* (whose number depends on the setup tested) are placed at each *floor* lateral side. With respect to the pathway length, the *servers* are tested in three different positions: halfway, a quarter, and an eighth of the *floor*. Thus, the first part of the pathways is intended to replicate the pedestrians' organization alongside the pathway side, being the *agents* attracted by the *servers* start points (Bernardini, Postacchini, et al., 2017). Concerning these start points' distances from the *floor* lateral edge, multiple setups are also tested in order to represent the classes of distance by literature (Bernardini, Postacchini, et al., 2017). Moreover, *servers* are connected through a single internal connection, the *dispatch*, to a single endpoint (placed near to the end of the pathway, at the *destination portal*). In this way, the configuration tries to force the *agents* to move near the *floor* edge by reproducing the maximum attraction phenomena for building-pedestrians distances of about 2m (Bernardini, Postacchini, et al., 2017).

The *agents'* motion is configurated so as to link them towards the *servers* placed on the same generation *floor* side, and then towards the final *destination portal*. In particular, the *agents* are divided between the elements of the *server* according to two distributions: homogeneous, where agents have the same of probability in choosing the related *server*, and by-literature, according to the real-world observations about the frequency for each class of distance from unmovable obstacles. The *dispatches* also increase the possibility of motion interaction between *agents* moving from the two start points to the unique endpoint. The *servers'* configuration also includes the following features:

1. *agents* are initially generated at the *entrance only portal*, and then directly move towards the exits [*approach: standard walk to target; Target: server exit*]. Each *server* influences the *agents'* motion as a waypoint for the evacuation motion, only because of its position (the *server* length is not relevant);
2. no limitations in the exit flows are considered [*Processors: unlimited; Capacity: infinite; Contact time: disabled*]. The impact of queueing phenomena on the *server* motion steps and at the exit can be reduced by combining these setup strategies to previous point 1.
3. the correct evacuation direction is identified uniquely to avoid coming-and-going behaviors and street-crossing behaviors along the *floor*, which are not noticed in flood evacuation conditions [*Dispatch objects* are configurated to directly connect the *servers* along the evacuation motion direction.

Each simulated *agent* moving on *floor* is characterized by a unique profile according to the *Agent Behaviour Tab* setup interface. Compact groups are simulated by considering no pre-movement time delay [*Population*: *arrival -> instant*]. The *agents'* maximum (e.g. capped) motion speed v_i is assigned through the *floor* properties (maximum speed allowed on the floor). The default speed-density relation is adopted since no current advances by literature on these aspects are provided for the flood evacuation case. The *agents'* queue spacing is similarly set up according to the default normal distribution (minimum=0m, maximum=1m, mode=0.25m, standard deviation 0.125m) for the same reason. The selected *direction bias* is “*none*” to avoid influencing the overtaking of other *agents*. Besides the configuration of *portals* and *servers*, the minimization of *floor*-crossing probability is also assigned to each *agent* [*assigned goal -> grouped: lowest cost*] hence representing an improved attraction behavior towards the *floor* limits where they are generated.

7. Appendix B

Setup symbol and property				
	A-B-C-D	H-L	2-4-8	R-S
Setup	Servers’ distance from the wall: “first servers” * // second server [m]	Probability a pedestrian can choose one of the “first servers” * [%]	First servers’ distance from the start of the pathway [m]	Entrance portals configuration: width; length; distance from the wall [m]
AH2R	1; 2 // 1	50; 50	43.5	3; 1; 0
AL2R	1; 2 // 1	29; 71	43.5	3; 1; 0
BH2R	0.5; 1.5 // 0.5	50; 50	43.5	3; 1; 0
BL2R	0.5; 1.5 // 0.5	29; 71	43.5	3; 1; 0
CL2R	0.5; 1.5; 2.5 // 0.5	29; 50; 21	43.5	3; 1; 0
DH2R	1; 2 // 0.5	50; 50	43.5	3; 1; 0
AH4R	1; 2 // 1	50; 50	21.75	3; 1; 0
AL4R	1; 2 // 1	29; 71	21.75	3; 1; 0
BH4R	0.5; 1.5 // 0.5	50; 50	21.75	3; 1; 0
BL4R	0.5; 1.5 // 0.5	29; 71	21.75	3; 1; 0

CL4R	0.5; 1.5; 2.5 // 0.5	29; 50; 21	21.75	3; 1; 0
DH4R	1; 2 // 0.5	50; 50	21.75	3; 1; 0
AH8R	1; 2 // 1	50; 50	10.87	3; 1; 0
AL8R	1; 2 // 1	29; 71	10.87	3; 1; 0
BH8R	0.5; 1.5 // 0.5	50; 50	10.87	3; 1; 0
BL8R	0.5; 1.5 // 0.5	29; 71	10.87	3; 1; 0
CL8R	0.5; 1.5; 2.5 // 0.5	29; 50; 21	10.87	3; 1; 0
DH8R	1; 2 // 0.5	50; 50	10.87	3; 1; 0
AH2S	1; 2 // 1	50; 50	43.5	3; 3; 1
AL2S	1; 2 // 1	29; 71	43.5	3; 3; 1
BH2S	0.5; 1.5 // 0.5	50; 50	43.5	3; 3; 1
BL2S	0.5; 1.5 // 0.5	29; 71	43.5	3; 3; 1
CL2S	0.5; 1.5; 2.5 // 0.5	29; 50; 21	43.5	3; 3; 1
DH2S	1; 2 // 0.5	50; 50	43.5	3; 3; 1
AH4S	1; 2 // 1	50; 50	21.75	3; 3; 1
AL4S	1; 2 // 1	29; 71	21.75	3; 3; 1
BH4S	0.5; 1.5 // 0.5	50; 50	21.75	3; 3; 1
BL4S	0.5; 1.5 // 0.5	29; 71	21.75	3; 3; 1
CL4S	0.5; 1.5; 2.5 // 0.5	29; 50; 21	21.75	3; 3; 1
DH4S	1; 2 // 0.5	50; 50	21.75	3; 3; 1
AH8S	1; 2 // 1	50; 50	10.87	3; 3; 1
AL8S	1; 2 // 1	29; 71	10.87	3; 3; 1
BH8S	0.5; 1.5 // 0.5	50; 50	10.87	3; 3; 1
BL8S	*0.5; 1.5 // 0.5*	*29; 71*	*10.87*	*3; 3; 1*
CL8S	0.5; 1.5; 2.5 // 0.5	29; 50; 21	10.87	3; 3; 1

DH8S	1; 2 // 0.5	50; 50	10.87	3; 3; 1

Table 11: Each setup (first column) is based on four properties coded by four symbols, and the properties characterization is discussed in each of the column, as also shown by to Table 1 criteria. Best setup in italics. Notes: * Each "first servers" group can be composed of two or three servers according to Section 2.4 criteria, so the semicolon separates the value for each of them.

8. Appendix C

SYMBOL	Meaning	REFERENCE
v_i	Evacuation speed	Equation 1
D_f	Floodwater depth	Equation 1
v_f	Floodwater speed	Equation 1
m_i	Pedestrian body mass	Equation 2
d_t	Time between two consecutive calculation iterations	Equation 2
O_g (t)	Drive-to-target force	Equation 2
$F_{rep,i}$	Repulsive force with surrounding pedestrians	Equation 2
$F_{rep,w}$	Repulsive force with surrounding obstacles	Equation 2
$F_{attr,i}$	Attractive force with surrounding pedestrians	Equation 2
$F_{attr,w}$	Attractive force with surrounding obstacles	Equation 2
R1, R2, R3	Setup groups having rectangular *portals*	Figure 1
S1, S2, S3	Setup groups having squared *portals*	Figure 1
A, B, C, D	Server position with respect to the wall	Figure 1 and Table 1
H, L	Probability a pedestrian can choose a server	Figure 1
2, 4, 8	Server position with respect to the start	Figure 1
R, S	Shape of the entrance portal	Figure 1
EC	Evacuation curves	Table 2

D_w	Pedestrian - side of the building distance during the evacuation	Table 2
t_{max}	Maximum evacuation time	Table 2
W	Waiting time percentage	Table 2
F	Evacuation flow	Table 2
SC	Secant cosine	Table 3
ERD	Euclidean relative difference	Table 3
EPC	Euclidean projection coefficient	Table 3
DAUC	Difference between the graphic Areas Under the Curves	Table 3

Table 12: list of notations and references to their detailed explanation